

# Thermal Evaluation of Masonry Shelf Angle Supports for Exterior-Insulated Walls

**Adam Di Placido, PE    Bailey Brown, PE    Drew Chong    Chris Schumacher**

## ABSTRACT

*Exterior insulation in above-grade wall assemblies is becoming more common as energy codes and voluntary energy efficiency programs continue to shift the building construction industry toward more stringent thermal performance standards. Exterior insulation can be effective for achieving high R-value walls; however, high-conductivity thermal bridges, such as cladding attachment systems, often penetrate the insulation and require careful consideration to avoid significantly degrading the insulation's thermal performance. Mitigating heat loss from cladding attachment systems is of great interest for heavyweight anchored masonry veneer claddings, which require a robust structural attachment system to transfer cladding loads back to the primary structure.*

*Masonry veneer claddings are typically supported by the building structure using a combination of intermittent anchors and shelf angle bearing supports. This paper discusses computer-based three-dimensional thermal modeling calibrated with physical testing of a shelf angle support to evaluate the thermal performance of shelf angle support design options available for exterior-insulated anchored masonry veneer walls. Calibration of the model demonstrated that the contact resistance between the shelf angle support and the structure can significantly reduce the associated heat loss. Additionally, this paper considers the impact of two other common thermal modeling oversights: circular cross-sectional area sizing and galvanized steel material property selection.*

*The calibrated thermal modeling results of this study demonstrate that shelf angle support designs can significantly diminish the effectiveness of the exterior insulation by 50%. Notable thermal improvements can be achieved by using more thermally efficient shelf angle supports designed specifically for reducing thermal transmittance. The calibrated thermal modeling results demonstrate that such products improve upon the thermal losses of traditional designs, reducing the effective R-value by approximately 15% when compared to an equivalent model with continuous insulation.*

*The results from this study demonstrate that with the appropriate selection of shelf angle support design, high R-value exterior-insulated masonry veneer walls are achievable.*

## INTRODUCTION

Insulation outboard of the above-grade wall backup structure (i.e., exterior insulation) is one strategy commonly used to meet the thermal performance compliance requirements of both mandatory and voluntary energy efficiency codes and standards. This method locates the insulation outboard of major structural elements, including the building's floor line structure and wall framing, thus potentially reducing the frequency and severity of thermal bridges through the insulation layer. Exterior insulation can also improve the durability and moisture management performance of the wall, particularly in colder climates where the risk for condensation to develop within the wall may be at its greatest. However, cladding loads must be transferred back to the backup wall structure, inevitably bridging the exterior insulation. Mitigating thermal bridging is thus a significant consideration for heavyweight cladding systems that rely on intermittent ties for lateral support and shelf angles or corbels for bearing support of the anchored

**Adam Di Placido** is a Building Science Engineer at RDH Building Science Inc, Seattle, Washington. **Bailey Brown** is an Associate at RDH Building Science Inc, Seattle, Washington. **Drew Chong** is a Building Science Engineer (EIT) at RDH Building Science Inc, Toronto, Ontario. **Chris Schumacher** is a Principal at RDH Building Science Inc, Waterloo, Ontario.

masonry veneer.

Many of the cladding attachment options available to lightweight and medium-weight cladding systems have been found to reduce the effective R-value (inclusive of thermal bridging) of the wall assembly anywhere from 5% to over 70% (Finch and Higgins 2018; Finch et al. 2013). Similarly, previous three-dimensional computer-simulated thermal modeling of exterior-insulated masonry veneer walls has found that thermal bridging due to masonry support systems can reduce the effective R-value of the wall assembly anywhere from 10% to over 60% (Finch and Higgins 2018; RDH Building Science Inc. 2016; Finch et al. 2013). This span in percent degradation considers various masonry ties and/or shelf angle support systems when used with different backup wall structures. Therefore, the use of a relatively heavyweight masonry veneer over an exterior-insulated backup wall does not necessarily mean that the thermal performance of the exterior insulation will be compromised, provided that thermal bridging at the attachment points is adequately managed.

Direct attachment of a shelf angle tight to the wall structure was found to reduce the thermal performance of the above-grade wall (inclusive of the wall structure, floor line, and masonry ties) by 40% to 55% (Finch et al. 2013). Alternatively, standing the shelf angle off the floor line structure with intermittent supports—such as structural steel knife plates, hollow steel section attachments, or proprietary brackets—has been found to reduce the effective R-value of the above-grade wall by a more manageable percentage: 12% to 22% (Finch et al. 2013).

The previous modeling efforts described above remain to be validated through physical thermal testing. This study provides validation of the modeled thermal performance of one proprietary shelf angle support option for exterior-insulated anchored masonry veneer walls and applies the calibrated modeling parameters to other common support options.

## **SHELF ANGLE SUPPORT SPECIMEN**

Thermal testing was performed on a proprietary intermittent shelf angle support bracket intended to be used with exterior insulation over a mass floor line structure. The hot-dip galvanized steel bracket was selected for this study for its ease of use, speed of installation in the field, and improved thermal performance over other non-proprietary shelf angle support options. Figure 1 depicts the C-like shaped bracket, which includes an inclined slot for anchor bolt attachment and triangular-perforated side walls. The support is typically spaced at 48 in. (1219 mm) and anchored to the floor line using an anchor bolt. The support is provided with an optional backside shim to accommodate construction tolerance; however, a shimmed attachment was not considered in this study.

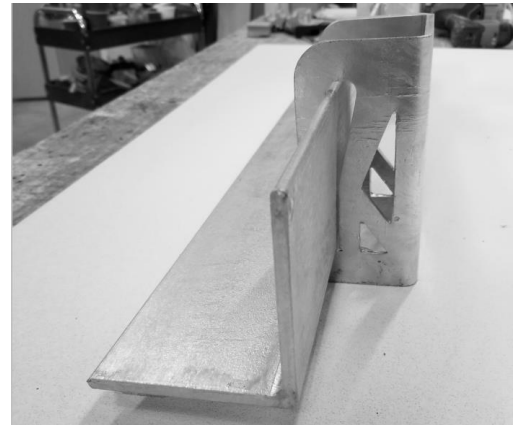


**Figure 1** A masonry shelf angle held by a proprietary support bracket.

## **PHYSICAL THERMAL TESTING**

Physical thermal testing was completed to calibrate the thermal modeling of the support using a modified ASTM C177 large-scale guarded hot plate apparatus (ASTM International 2019). The hot plate apparatus used for this study measures heat flow across a horizontally oriented assembly specimen. The apparatus consists of a cold plate (at top) and multiple hot plates (at bottom) to induce a temperature differential across the assembly. The apparatus accommodates a 48 in. (1219 mm) square assembly with the heat flow across the assembly being measured at the 16 in. (406 mm) square metered hot plate, called the meter plate, at the center of the apparatus. Heat flow across the specimen is measured by the power input to the meter plate, which is guarded at the sides and below with guard plates. The guard plates are maintained at the same temperature to thermally isolate the meter plate from the ambient conditions.

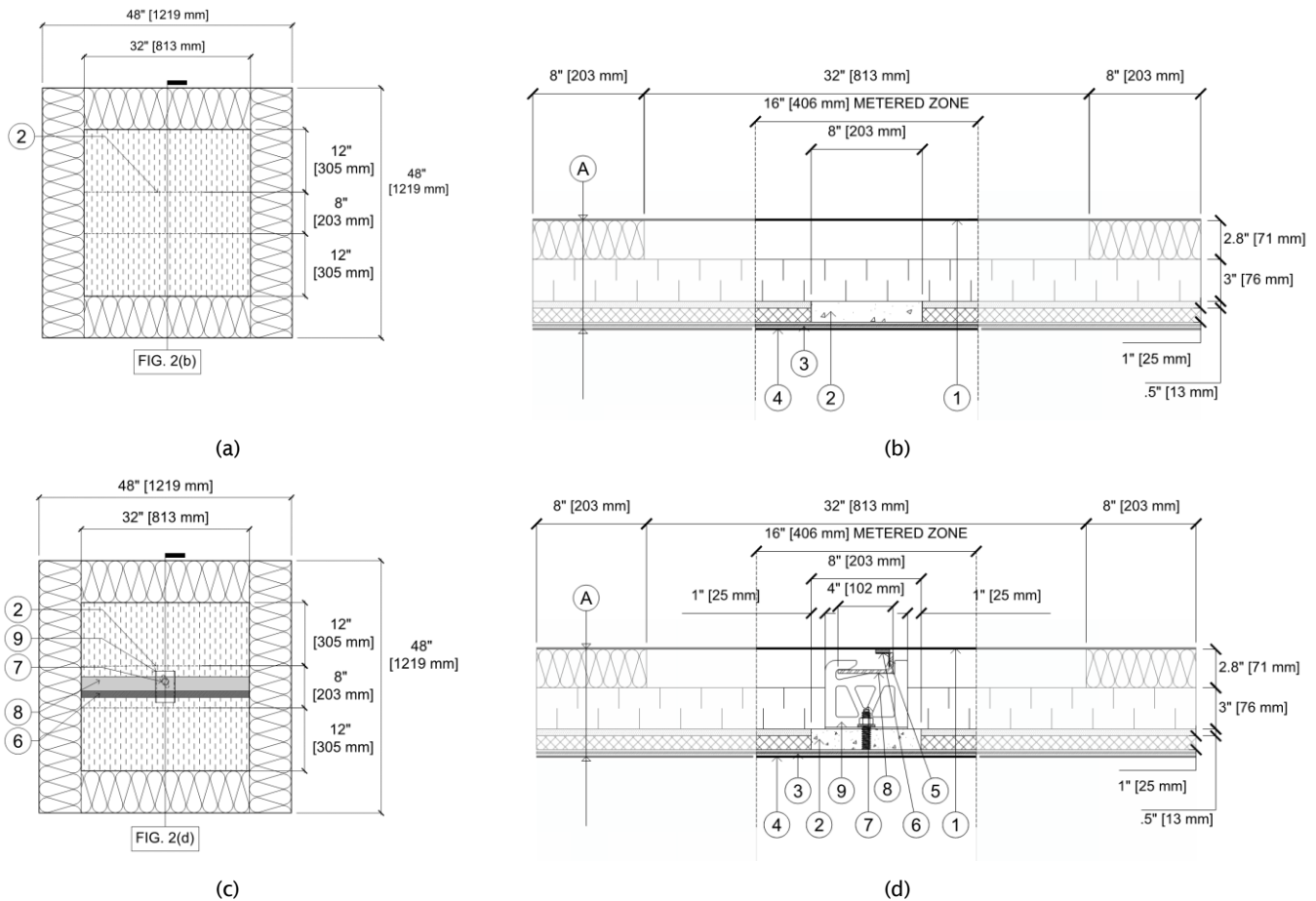


**FIGURE 2 LEGEND:**

1. COLD PLATE
2. CONCRETE PAVER
3. POLYETHYLENE FOAM
4. METER (HOT) PLATE
5. SMALL STEEL ANGLE
6. POLYETHYLENE FOAM
7. THREADED ROD WITH SQUARE WASHER, ROUND WASHER, AND NUT
8. SHELF ANGLE
9. SHELF ANGLE SUPPORT BRACKET

**ASSEMBLY A (TOP TO BOTTOM):**

- COLD PLATE
- FIBERGLASS BATT INSULATION
- MINERAL WOOL INSULATION
- FIBERGLASS MAT FACED GYPSUM SHEATHING
- XPS INSULATION
- POLYETHYLENE FOAM
- GUARD (HOT) PLATE

**Figure 2** Schematic of the mockup assemblies. (a) Plan view with continuous insulation. (b) Section with continuous insulation. (c) Plan view with bracket. (d) Section with bracket. Plans and sections are not to scale.

Two mockup assemblies were tested using the apparatus (see Figure 2): one including continuous exterior insulation and one including the shelf angle support bridging the exterior insulation layer. A concrete slab edge condition was approximated for both assemblies using a 1-1/2 in. (38 mm) thick, 8 in. (203 mm) wide, 32 in. (813 mm) long concrete paver. The shelf angle support bracket was attached to the paver using a 5/8 in. (16 mm) diameter threaded rod grouted into the concrete paver. Extruded polystyrene (XPS) insulation measuring 1 in. (25 mm) thick covered by a 1/2 in. (13 mm) thick fiberglass mat faced gypsum sheathing board was used to approximate a simplified framed wall assembly above and below the floor slab. The mockup assembly was exterior insulated with 3 in. (76 mm) of mineral wool insulation. An air cavity that occurred between the mineral wool insulation and the cold plate was filled at the perimeter with an 8 in. (203 mm) wide band of fiberglass batt guard insulation to limit lateral heat flow. For simplicity of construction, a masonry veneer was not included in either mockup, and the hot-dip galvanized steel

ledger angle used with the bracket was ripped to fit the depth of the apparatus. A polyethylene foam layer was used where rigid materials were in contact with the hot and cold plates to approximate vertical air film resistances.

Hot plate testing is not typically used to measure heat flow across nonhomogeneous or thermally bridged samples due to the potential for temperature gradients to develop along the hot and cold plates and for lateral heat fluxes to develop through the specimen toward the sides of the apparatus (ASTM International 2019). To address these concerns, this study implemented the following three methods:

1. Temperature gradients that developed due to thermal bridging and the nonhomogeneity of the specimen were assessed using a greater number of temperature sensors on the hot and cold plates than required by the standard as well as with added temperature sensors at the mockup specimen.
2. Polyethylene foam was used between the mockup surfaces and the hot and cold plates to encourage lateral distribution of heat in the plane of the plates and more uniform temperatures at the plates. The contact resistance imparted by the polyethylene foam material was previously measured and calibrated by Straube, Simonji, and Schumacher (2019) and was selected to approximate air film resistances for vertical surfaces.
3. The concrete paver and steel shelf angle measured 32 in. (813 mm) in length, which exceeded the width of the 16 in. (406 mm) wide meter plate but did not reach the 48 in. (1219 mm) width of the apparatus. Perimeter guard insulation was installed at the ends of the paver and the angle to limit lateral heat losses.

Further information regarding the test apparatus and the commissioning test program used to validate its use for thermally bridged specimens can be found in the paper titled “Thermal Resistance Measurement of Two- and Three-D Thermal Bridges Using an ASTM C177-based Apparatus” in these conference proceedings (Straube et al. 2019) and the engineering master’s thesis of Joseph Simonji (2016).

## **PHYSICAL TESTING RESULTS**

After the mockup assembly was inserted into the apparatus, the hot and cold plates were set to 87.6°F (30.9°C) and 62.4°F (16.9°C), respectively, until the assembly reached an equilibrium condition (no variations in the power draw at the meter plate within 1%). The power draw at the hot meter plate was used to determine the steady-state heat flow across the test area. The total heat flow measured across the continuously insulated assembly and across the mockup assembly with the shelf angle support bracket was 2.743 BTU/hr (0.804 W) and 8.889 BTU/hr (2.605 W), respectively. The difference between these two heat flows was used to determine the point thermal transmittance value of the thermal bridge created by the support under the test conditions, which was 0.244 BTU/°F·hr (0.129 W/K). It should be noted, however, that this point transmittance value is representative of the mockup assembly with the shelf angle support bracket and may not be indicative of the bracket’s transmittance value when installed on an actual floor line structure due to different wall constructions, the presence of air and water control layer membranes, and other project specific construction variables.

## **THERMAL MODELING CALIBRATION**

The two mockup assemblies were modeled using the HEAT3 software to compare the theoretical modeling results to the physical test performance. HEAT3 is an EN ISO 10211 validated three-dimensional conductive heat transfer software package (Blocon 2018). Material conductivity values, except for the concrete paver and the polyethylene foam, were obtained from ASHRAE Handbook—Fundamentals (2017), NFRC 101 (2016), and manufacturer-reported thermal performance values. As previously stated, the resistance provided by the polyethylene foam was measured and calibrated by a previous study (Straube et al. 2019). The conductivity of the concrete paver was measured using the transient line source method per the ASTM D5334 standard and was found to be 0.734 BTU/hr·ft·°F (1.27 W/m·K) for the tested sample (ASTM International 2014). This resulted in good agreement (1.8%

difference) between the modeled and tested heat flow for the mockup with continuous insulation.

The thermal model of the mockup with the shelf angle support bracket was also found to be in good agreement (4.1% difference) with the tested heat flow value. This agreement allowed for exploration of three model parameters and their impact on the total heat flow: the circular threaded rod section, the conductivity of the steel support, and the contact resistance between the highly conductive support and the concrete substrate. The relative influence of each of these parameters is summarized in Table 1 as a percentage difference from the tested heat flow and the calibrated model, and the three parameters are discussed in further detail in the following sections.

**Table 1. Comparison of Thermal Model Results to Thermal Testing**

	Total Heat Flow	% Difference from Tested	% Difference from Calibrated Model
Tested Assembly with Support	<b>8.889 BTU/hr (2.605 W)</b>	-	-4.1%
Calibrated Thermal Model	9.254 BTU/hr (2.712 W)	4.1%	-
Parameter 1: Circular Cross-Sectional Areas	9.428 BTU/hr (2.763 W)	6.1%	1.9%
Parameter 2: Conductivity of Steel Section	9.772 BTU/hr (2.864 W)	9.9%	5.6%
Parameter 3: Contact Resistance	10.175 BTU/hr (2.982 W)	14.5%	10.0%

### Parameter 1: Circular Cross-Sectional Areas

One limitation of the modeling software used for this study is that only rectangular geometries can be modeled such that small circular components (e.g., fasteners) must be approximated with square prisms. Fastener sections are commonly sized such that 1) the modeled fastener section is a square with lengths equal to the fastener's actual diameter, 2) the section is sized as a square with an area equal to the area of the actual fastener section, or 3) the fastener's modeled surface area is sized equal to the actual fastener. Sizing fasteners to the square of the fastener diameter is considered a conservative approach because it overstates the area of the thermal bridge. Sizing circular materials using an equivalent sectional area or equivalent surface area approach provides a more accurate representation of the modeled heat transfer. The equivalent sectional area approach is generally more accurate when the section is in contact with other solid materials and the primary direction of heat transfer is perpendicular to the section. The equivalent surface area approach is generally more accurate when the circular component is surrounded by a fluid, such as air, because the heat transfer is largely driven by the surface area of the solid-fluid boundary. Given that the majority of the fastener under study is embedded in solid concrete and that the direction of heat transfer is primarily parallel to the axis of the fastener, fastener geometry in the calibrated model was sized using the equivalent sectional area approach. If the fastener area had been increased such that the side of the square fastener equaled the fastener's diameter, a minor increase in the total heat flow (approximately 2%) would have resulted, as shown in Table 1, Parameter 1. It should also be noted that the hexagonal nut at the fastener head is surrounded by an air cavity, and therefore it may be more accurate to model the nut as an equivalent surface area; however, sizing the nut using the equivalent sectional area or equivalent surface area approach did not result in any appreciable difference (less than 0.1%) in the modeled heat flow.

### Parameter 2: Conductivity of Steel Sections

The shelf angle support bracket tested is composed of 0.185 in. (4.7 mm) thick galvanized steel. Industry standard sources report a material conductivity of 35.8 BTU/hr•ft°F (62.0 W/m•K) for galvanized sheet metal and 26.2 BTU/hr•ft°F (45.3 W/m•K) for mild steel (ASHRAE 2017, NFRC 2016). The conductivity of galvanized sheet metal is significantly greater due to the galvanized coating. Therefore, the thicker the sheet metal, the less influence the galvanized coating will have on the overall conductivity, and the conductivity will approach the value for mild steel. The conductivity value for mild steel was assumed for the bracket in the calibrated model to provide agreement with the tested results. If the conductivity for galvanized sheet metal had been used, the modeled heat flow would

have increased by approximately 6%, as shown in Table 1, Parameter 2.

### Parameter 3: Contact Resistance

Contact resistances are not typically included in thermal modeling; however, many have noted that contact resistances can be significant where highly conductive materials interface (e.g., ASHRAE 2017, Morrison Hershfield 2011, McGowan and Desjarlais 1995). ASHRAE Handbook—Fundamentals (2017) advises that contact resistances between metal building structures may range anywhere from R-0.06 (0.01 RSI) to R-0.6 (0.1 RSI); however, it does not provide guidance regarding the precise selection of contact resistances or reasonable values between nonmetal materials. Most of the existing body of research regarding contact resistances for buildings has focused on light-gauge, steel-framed walls. McGowan and Desjarlais (1995) found that using a contact resistance of R-0.20 (0.035 RSI) at the interface between light-gauge steel studs and gypsum sheathing resulted in good agreement between modeled and tested performance, and that excluding the contact resistance in the model could account for up to a 10% difference in the effective R-value. Another study also found good agreement using a similar contact resistance for steel-framed assemblies (Morrison Hershfield 2011). The researchers also found good agreement between modeled and physical testing when assuming a contact resistance of R-0.011 (0.002 RSI) at steel-to-steel connections and R-0.057 (0.010 RSI) at steel-to-concrete interfaces at a variety of different assemblies and details (Morrison Hershfield 2011).

For this study, a contact resistance of R-0.06 (0.011 RSI) was included in the final calibration between the support and the concrete, and a value of R-0.01 (0.0018 RSI) was included at the points of contact between the shelf angle and support. These contact resistances provided good agreement between the tested and modeled heat flow, offering further validation of the contact resistances used by others (Morrison Hershfield 2011). The Parameter 3 result in Table 1 excludes all contact resistances, thus indicating that the contact resistances are significant, accounting for approximately 10% of the difference between the modeled and tested heat flow.

In most practical field applications, the shelf angle support is installed over a water-resistive barrier (WRB) membrane rather than directly to the concrete slab edge, as was tested. Therefore, including the contact resistance between steel and bare concrete may not be appropriate for evaluating the in situ thermal performance of the shelf angle supports. To determine the relative influence of WRB membranes on the thermal performance of the bracket, models were developed for an 8 in. (203 mm) thick concrete slab edge condition with 4 in. (102 mm) of exterior mineral wool insulation and a masonry veneer. The models considered the small resistance provided by a 20 mil (0.51 mm) silicone-based liquid-applied WRB membrane, a 40 mil (1 mm) styrene-butadiene-styrene (SBS) self-adhered membrane (SAM), and the calibrated contact resistance with bare concrete in comparison. These three cases were compared to a model that did not consider contact resistances or membranes. Table 2 presents the resulting point transmittance values and effective R-values. The concrete contact resistance significantly improved the thermal performance of the bracket (8.9% increase in the effective R-value). The impact of the WRB membrane and SAM resistance was more modest, offering a 2%–3% increase in the effective R-value; however, it should be noted that the contact resistances assumed for the WRB membrane and SAM resistances remain to be validated through physical testing. To ensure that the thermal evaluation offered by this study is applicable to a wide range of real-world applications while also erring on the side of conservatism, the remainder of the modeling results reported in this study include the WRB membrane (R-0.009/0.00016 RSI) behind the shelf angle support.

**Table 2. Comparison of Modeled Bracket Performance with Various Back Resistances**

	Point Transmittance BTU/°F·hr (W/K)	% Difference	Effective R-Value (RSI)	% Difference
No Contact Resistances	<b>0.359 (0.189)</b>	-	<b>5.28 (0.930)</b>	-
WRB Membrane (R-0.009/0.00016 RSI)	0.349 (0.184)	-2.8%	5.38 (0.947)	1.9%
SAM (R-0.016/0.0028 RSI)	0.343 (0.181)	-4.5 %	5.45 (0.960)	3.2%
Concrete Contact Resistance (R-0.06/0.01 RSI)	0.317 (0.167)	-11.7 %	5.75 (1.013)	8.9%

## THERMAL MODELING RESULTS

Results from the calibration of the masonry shelf angle bracket model were used to develop a series of models to evaluate the thermal performance of exterior-insulated anchored masonry bearing support options. The material conductivity values assumed for the models are listed in Table 3. Standard air film resistances from *ASHRAE Handbook—Fundamentals* (2017) were applied at interior and exterior surfaces and are included where effective R-values are listed.

**Table 3. Material Thermal Conductivity Values**

Material	Conductivity (BTU/hr•ft°F)	Conductivity (W/m•K)	Source
Clay Brick <sup>1</sup>	0.463	0.800	(ASHRAE 2017)
Steel - Galvanized Sheet (0.14% C)	35.8	62.0	(NFRC 2016)
Steel - Carbon (Mild)	26.2	45.3	(ASHRAE 2017)
Cast-in-Place Concrete <sup>2</sup>	1.45	2.50	(ASHRAE 2017)
Mineral Wool	0.020	0.034	(ASHRAE 2017)
1 in. (25 mm) Air Space Behind Masonry <sup>3</sup>	0.085	0.147	(ASHRAE 2017)
4.8 in. (122 mm) Air Space at Bracket <sup>3</sup>	0.43	0.75	(ASHRAE 2017)
Exterior Gypsum Sheathing	0.075	0.129	Manufacturer's data sheet
Interior Gypsum Wallboard	0.093	0.160	(ASHRAE 2017)
Silicone-Based WRB	0.19	0.32	(NFRC 2016)

<sup>1</sup>Assuming a density between 110 and 120 lbs/ft<sup>3</sup> (1760 and 1920 kg/m<sup>3</sup>)

<sup>2</sup>Assuming normal-weight concrete

<sup>3</sup>Assuming a mean temperature of 50°F (10°C), a temperature differential of 30°F (16.7°C), and emissivity of 0.8

Three configurations for the shelf angle support were modeled: direct to the slab edge with a large 0.25 in. (6.35 mm) thick shelf angle; intermittent brackets (without punched perforations) fabricated from 0.187 in. (4.76 mm) thick steel to stand off the shelf angle from the structure; and intermittent brackets with perforations fabricated from 0.187 in. (4.76 mm) thick steel (similar to the tested bracket configuration). These configurations are illustrated in Figure 3. Although cross-cavity flashings are typically located at shelf angle locations, flashing elements bridging the exterior insulation were excluded from this study due to the variability of flashing materials and methods commonly used in practice. The brackets are assumed to be spaced at 48 in. (1219 mm) on-center for the standoff models. The shelf angles are attached to an 8 in. (203 mm) thick concrete slab edge with a 20 mil (0.51 mm) WRB membrane (R-0.009/0.00016 RSI). Modeling was completed for 4 in. (102 mm) of exterior mineral wool insulation to represent typical construction conditions.

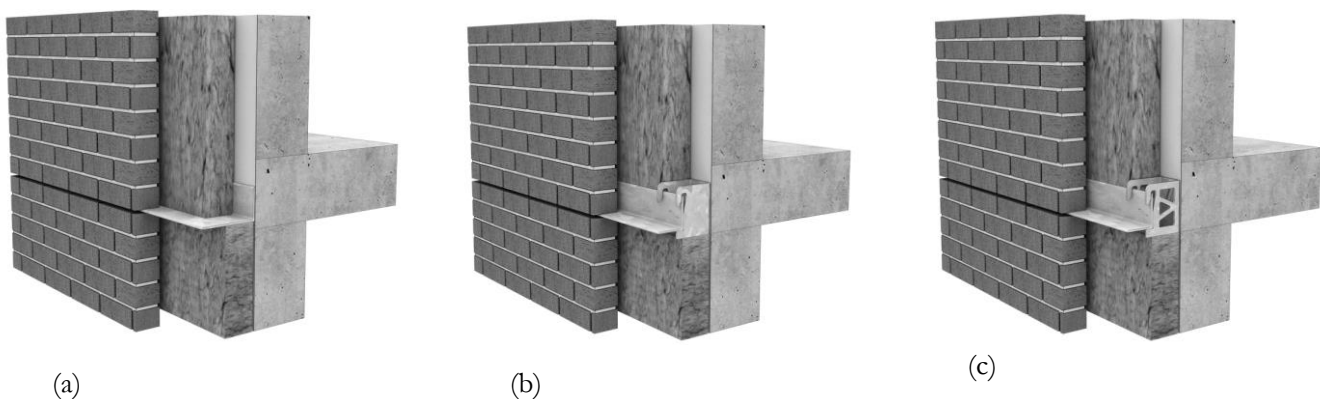


**Figure 3** Schematic of (a) direct shelf angle attachment, (b) shelf angle standoff with nonperforated bracket, and (c) shelf angle standoff with perforated bracket.

Table 4 presents the resulting linear transmittance ( $\Psi$ -value), effective R-values, and percent reduction of the R-value when compared to an identical slab edge condition with continuous exterior insulation (i.e., no thermal bridging). The effective R-values are reported for both the floor line condition alone (excluding the walls above and below) and including a 4 ft (1.2 m) tall wall above and below the 8 in. (203 mm) concrete slab edge for a floor-to-floor height of 8.33 ft (2.54 m). Thermal bridging from masonry ties was not considered for this study. The shelf angle attached directly to the floor structure created a large, continuous thermal bridge through the exterior insulation, degrading the effective R-value by over 90% at the floor line and almost 50% across the full height wall. Standing the shelf angle off the wall using nonperforated intermittent bracket supports significantly reduced thermal bridging, increasing the effective R-value four-fold at the floor line and approximately 65% across the full height wall. Using a bracket with punched perforations to reduce the steel area bridging the insulation further improved the floor line effective R-value by approximately 14% and the effective R-value of the full height wall by approximately 3%.

**Table 4. Modeled Thermal Performance of Various Shelf-Angle Support Options**

	Direct Attachment (Large Angle)	Bracket (Standoff) Without Perforations	Bracket (Standoff) With Perforations
$\Psi$ -value BTU/ft <sup>2</sup> ·°F·hr (W/m <sup>2</sup> ·K)	0.449 (0.776)	0.092 (0.160)	0.077 (0.133)
Effective R-Value (Floor Line Only)	R-1.37 (RSI 0.24)	R-5.17 (RSI 0.91)	R-5.88 (RSI 1.04)
R-Value Reduction (Floor Line Only)	92.5%	71.7%	67.8%
Effective R-Value (With Walls)	R-9.93 (RSI 1.75)	R-16.35 (RSI 2.88)	R-16.83 (RSI 2.96)
R-Value Reduction (With Walls)	49.5%	16.8%	14.4%

## CONCLUSION

A thermal model of an intermittent shelf angle support bracket with exterior insulation was calibrated using physical testing results from a guarded hot plate apparatus. Careful selection of the conductivity of steel sections and contact resistances was required to provide agreement between modeled and tested results. Contact resistances were found to have a significant impact on the heat flow through the bracket by providing a small thermal break, suggesting that previous modeling efforts that ignored these small resistances may have overestimated heat losses at shelf angle supports.

Contact between the shelf angle support and a WRB membrane at the concrete floor line structure provided some thermal improvement compared to attaching the shelf angle support directly to the concrete without contact resistances. However, the small resistance provided by the membrane was not found to be as impactful as the contact resistance with bare concrete. Further work is required to validate the membrane resistances assumed in this study and to assess the influence of common WRB membranes on the thermal performance of shelf angle support options.

The calibrated model results presented here reaffirm previous thermal evaluation studies of exterior-insulated masonry walls. Shelf angle standoffs, such as the intermittent brackets evaluated in this study, offer more manageable reductions to the effective R-values than shelf angles attached direct to the structure. These results further justify the continued use of the standoff approach for the attachment of masonry shelf angles and the development of easily accessible, cost-effective commercial solutions.

## REFERENCES

- ASHRAE. 2017. *2017 ASHRAE Handbook—Fundamentals*. Atlanta, GA: American Society of Heating, Refrigerating and Air-Conditioning Engineers (ASHRAE).
- ASTM International. 2014. *ASTM D5334-14, Standard Test Method for Determination of Thermal Conductivity of Soil and Soft Rock by Thermal Needle Probe Procedure*. West Conshohocken, PA: ASTM International.
- ASTM International. 2019. *ASTM C177-19, Standard Test Method for Steady-State Heat Flux Measurements and Thermal Transmission Properties by Means of the Guarded-Hot-Plate Apparatus*. West Conshohocken, PA: ASTM International.
- Blocon. 2018. <https://buildingphysics.com/heat3-3/>. Accessed April 22, 2019.

- Finch, G., and J. Higgins. 2018. *Cladding Attachment Solutions for Exterior-Insulated Commercial Walls*. RDH Building Science Inc.
- Finch, G., M. Wilson, and J. Higgins. 2013. "Thermal Bridging of Masonry Veneer Claddings & Energy Code Compliance." *12th Canadian Masonry Symposium*. Vancouver, BC.
- McGowan, A.G., and A.O. Desjarlais. 1995. "A Comparison of Thermal Bridging Calculation Methods." *Proceedings of the Thermal Performance of the Exterior Envelopes of Buildings VI*. Atlanta, GA: American Society of Heating, Refrigerating and Air-Conditioning Engineers (ASHRAE).
- Morrison Hershfield. 2011. "Thermal Performance of Building Envelope Details for Mid- and High-Rise Buildings (1365-RP)." Vancouver, BC.
- NFRC. 2016. *NFRC 101-2017 Procedure for Determining Thermophysical Properties of Materials for Use in NFRC-Approved Software*. Greenbelt, MD: National Fenestration Rating Council Incorporated.
- RDH Building Science Inc. 2016. *2016 Masonry Systems Guide: Northwest Edition*. Northwest Masonry Institute & Masonry Institute of Washington.
- Simonji, J. "Development and Commissioning of a Large-Scale Rotatable Guarded Hot Plate Apparatus." Master's thesis, University of Waterloo, 2016.
- Straube, J., J. Simonji, and C. Schumacher. 2019. "Thermal Resistance Measurement of Two- and Three-D Thermal Bridges Using an ASTM C177-based Apparatus." *These Conference Proceedings*.